Title

Cognitive relevance of an evolutionarily new and variable prefrontal structure

Authors and affiliations

Ethan H. Willbrand[1,2], Samantha Jackson[2], Szeshuen Chen[1], Catherine B. Hathaway[3], Willa I. Voorhies[1], Silvia A. Bunge[1,2*], Kevin S. Weiner[1,2*]

[1]Department of Psychology, University of California, Berkeley, Berkeley, CA, 94720 USA

[2]Helen Wills Neuroscience Institute, University of California, Berkeley, Berkeley, CA, 94720 USA

[3]Cognitive Science, University of California, Berkeley, Berkeley, CA 94720 USA

**Co-senior authors*

Corresponding author: Kevin S. Weiner

Email: kweiner@berkeley.edu

Keywords*:* neuroanatomy, MRI, sulcal morphology, reasoning, comparative biology, lateral prefrontal cortex

Abstract

Identifying structural-functional correspondences is a major goal among biologists. In neurobiology, recent findings identify relationships between performance on cognitive tasks and the presence or absence of small, shallow indentations, or sulci, of the human brain. Here, we tested if the presence or absence of one such sulcus, the paraintermediate frontal sulcus (pimfs-v) in lateral prefrontal cortex, was related to relational reasoning in young adults from the Human Connectome Project (ages 22-36). After manually identifying 2,877 sulci across 144 hemispheres, our results indicate that the presence of the pimfs-v in the left hemisphere was associated with a 21-34% higher performance on a relational reasoning task. These findings have direct developmental and evolutionary relevance as recent work shows that the presence or absence of the pimfs-v is also related to reasoning performance in a pediatric cohort, and that the pimfs-v is exceedingly rare in chimpanzees. Thus, the pimfs-v is a novel developmental, cognitive, and evolutionarily relevant feature that should be considered in future studies examining how the complex relationships among multiscale anatomical and functional features of the brain give rise to abstract thought.

Introduction

Identifying structural-functional correspondences is a major goal across subdisciplines in the biological sciences. In neurobiology and cognitive neuroscience, there is broad interest in uncovering relationships between neuroanatomical features of the human brain and cognition — especially for structures in parts of the brain that are largely human-specific. Given that 60-70% of the human cerebral cortex is buried in indentations, or sulci [1–3], there continues to be great interest in the relationships among sulcal morphology, functional representations, and cognition. Previous work exploring this relationship has largely focused on the consistent and prominent sulci within primary sensory cortices, such as the central and calcarine sulci [4–11]. Nevertheless, recent work has begun to explore the less consistent and more variable sulci, such as small and shallow sulci in association cortices that are not always present in a given hemisphere. For example, recent studies have identified relationships between the presence or absence of specific sulci in association cortices and individual differences in human cognitive abilities and clinical conditions (for review see [12]), which could be mediated by differences in white matter architecture in relation to these sulcal features [3,13–15].

To date, relationships between the presence/absence of variable sulci and cognition have been most widely explored in the anterior cingulate cortex (ACC) [12]; here, we focus on variations in the folding of the lateral prefrontal cortex (LPFC), a highly expanded region crucial for higher-level functions such as abstract reasoning [16–22]. A combination of previous findings [23–25] further motivated the present study, showing that a sulcus in anterior LPFC (ventral para-intermediate frontal sulcus, pimfs-v) was variably present in children and adolescents [23,24] and markedly rare in chimpanzees [25]. Further, the presence of left hemisphere pimfs-v in a sample of 6-18-year-olds was associated with higher reasoning scores [24]. Building on these previous results in the present study, we show that the sulcal patterning of the pimfs and the relationship between the presence/absence of the pimfs-v and reasoning is a reliable and enduring individual difference generalizing to an adult sample (ages 22-36). The reliable brain-behavior relationship between the presence of the left pimfs-v and reasoning across age groups and studies is important given a timely discussion among researchers regarding the reliability of brain-behavior relationships [26–28]. We discuss these findings in the context of (i) the role of anterior LPFC and reasoning across age groups and (ii) hypothesized relationships among the presence/absence of sulci, the morphology of sulci, white matter architecture, and the efficiency of network communication contributing to performance on cognitive tasks.

Materials and Methods

(a) Participants

Data for the young adult human cohort analyzed in the present study were taken from the Human Connectome Project (HCP) database (https://www.humanconnectome.org/study/hcp-young-adult/overview). Here we used 72 participants (50% female, aged between 22 and 36 years old). These participants have also been used in our previous work [29,30].

(b) Imaging data acquisition

Anatomical T1-weighted (T1-w) MRI scans (0.7 mm voxel resolution) were obtained in native space from the HCP database. First, the images obtained from the scans were averaged. Then, reconstructions of the cortical surfaces of each participant were generated using FreeSurfer, a software used for processing and analyzing human brain MRI images (v6.0.0, surfer.nmr.mgh.harvard.edu). All subsequent sulcal labeling and extraction of anatomical metrics were calculated from the cortical surface reconstructions of individual participants generated through the HCP's custom-modified version of the FreeSurfer pipeline [31–33].

(c) Behavioral data

(i) *Overview*

In addition to structural and functional neuroimaging data, the Human Connectome project also collected a wide range of behavioral metrics (motor, cognitive, sensory, and emotional processes) from the NIH toolbox [34] that illustrate a set of core functions relevant to understanding the relationships between human behavior and the brain (for task details see: https://wiki.humanconnectome.org/display/PublicData/HCP-YA+Data+Dictionary-+Updated+for+the+1200+Subject+Release#HCPYADataDictionaryUpdatedforthe1200SubjectRelease-Instrument). 71 of 72 participants in the present project had behavioral scores. Below we describe the three behavioral tests used.

(ii) *Reasoning task*

The ability to reason about the patterns, or relations, among disparate pieces of information has long been recognized as central to human reasoning and learning (e.g., [35–37]). Tests of relational reasoning assess the ability to integrate and generalize across multiple pieces of information; as a result, they help to predict real-world performance in a variety of domains [38]. Here, we used the behavioral data obtained for each participant measuring reasoning skills using a measure of relational reasoning, the Penn Progressive Matrices Test from the NIH toolbox [34]. This test is highly similar to the classic Raven's Progressive Matrices [39], WISC-IV Matrix Reasoning task [40], and other task variants that are ubiquitous in assessments of so-called "fluid intelligence." Participants must consider how shapes in a stimulus array — a 2x2, 3x3, or 1x5 arrangement of squares, in the case of the current task — are related to one another (e.g., an increase, across a row or column, in the number of lines superimposed on a shape) [41–46]. Specifically, participants must extrapolate from the visuospatial relations present in the array and select among five options the shape that completes the matrix. The task is composed of 24 different matrices to complete, in order of increasing difficulty. Testing is discontinued after five incorrect choices in a row, and the total score is calculated.

(iii) *Processing speed task*

To measure processing speed, participants completed the Pattern Comparison Processing Speed Test from the same NIH toolbox [34]. This test has been designed to measure the speed of cognitive processing based on the participant's ability to discern as quickly as possible whether two adjacent pictures are identical. In this test, participants must consider several possible differences (addition/removal of an element or the color or number of elements on the pictures). They indicate via a yes-no button press whether the two stimuli are identical, and their final score corresponds to the number of trials answered correctly during a 90-second period.

(iv) *Working memory task*

To measure working memory performance, participants completed the List Sorting Working Memory Test from the NIH toolbox [34]. In this task, each participant sequences different visually and orally presented stimuli (alongside a sound clip and written text for the name of the item) in two conditions: 1-List and 2-List. In the former, participants order a series of objects (food or animals) from smallest to largest. In the latter, participants are presented with both object groups (food and animals) and must report the food in size order and then the animals in size order. Crucially, completing this task not only requires working memory manipulation and maintenance but also relational thinking, given that it also requires participants to assess the relationship between the different stimuli. To report the items in size order it is necessary to compare pairs of stimuli and then engage in transitive inference across pairs (e.g., as reported by [47,48]).

(d) <u>Morphological analyses</u>

(i) Cortical surface reconstruction

FreeSurfer's automated segmentation tools [31,32,49] were used to generate cortical surface reconstructions. Briefly, each anatomical T1-w image was segmented to separate gray from white matter, and the resulting boundary was used to reconstruct the cortical surface for each participant [31,50]. Each reconstruction was visually inspected for segmentation errors, and these were manually corrected when necessary.

Cortical surface reconstructions facilitate the identification of shallow tertiary sulci compared to post-mortem tissue – for two main reasons. First, T1-w MRI protocols are not ideal for imaging vasculature; thus, the vessels that typically obscure the tertiary sulcal patterning in post-mortem brains are not imaged on standard-resolution T1-w MRI scans [30,51]. Indeed, indentations produced by these smaller vessels that obscure the tertiary sulcal patterning are visible in freely available datasets acquired at high field (7T) and micron resolution (100–250 µm) [52,53]. Thus, the present resolution of our T1s (0.7 mm isotropic) is sufficient to detect the shallow indentations of tertiary sulci yet is not confounded by smaller indentations produced by the vasculature. Second, cortical surface reconstructions are created from the boundary between gray and white matter; unlike the outer surface, this inner surface is not obstructed by blood vessels [51,54].

(ii) ***Defining the presence and prominence of the para-intermediate middle frontal sulcus***

Individuals typically have anywhere from three to five tertiary sulci within the middle frontal gyrus (MFG) in LPFC [23,30,55,56]. The posterior MFG contains three of these sulci, which are present in all participants: the anterior (pmfs-a), intermediate (pmfs-i), and posterior (pmfs-p) components of the posterior middle frontal sulcus (pmfs). In contrast, the tertiary sulcus within the anterior MFG, the para-intermediate middle frontal sulcus (pimfs), is variably present. A given hemisphere can have zero, one, or two pimfs components (examples in **figure 1**). As described in prior work [24,57,58], the dorsal and ventral components of the pimfs (pimfs-d and pimfs-v) were generally defined using the following two-fold criterion: i) the sulci ventrolateral to the horizontal and ventral components of the intermediate middle frontal sulcus, respectively, and ii) superior and/or anterior to the mid-anterior portion of the inferior frontal sulcus.

We first manually defined the pimfs within each individual hemisphere with *tksurfer* [30]. Manual lines were drawn on the *inflated* cortical surface to define sulci based on the most recent schematics of pimfs and sulcal patterning in LPFC by Petrides [57], as well as by the *pial* and *smoothwm* surfaces of each individual [30]. In some cases, the precise start or end point of a sulcus can be difficult to determine on a surface [59]. Thus, using the *inflated*, *pial*, and *smoothwm* surfaces to inform our labeling allowed us to form a consensus across surfaces and clearly determine each sulcal boundary. For each hemisphere, the location of the pimfs was confirmed by three trained independent raters (E.H.W., S.M., S.C.) and finalized by a neuroanatomist (K.S.W.). Although this project focused on a single sulcus, the manual identification of all LPFC sulci (2,877 sulcal definitions across all 72 participants) was required to ensure the most accurate definitions of the pimfs components. For in-depth descriptions of all LPFC sulci, see [23,30,55–57,60]. The incidence rates of the two pimfs components (i.e., sulcal patterning) were compared within and between hemispheres with Chi-squared and Fischer exact tests, respectively. Chi-squared tests were carried out with the chisq.test function from the stats R package [all statistical tests were implemented in R (v4.0.1; https://www.r-project.org/)]. Fisher's exact tests were carried out with the fisher.test function from the stats R package.

(e) Behavioral analyses: Relating the presence of the pimfs to reasoning performance

Participant age and gender were not considered in these analyses, as they were not associated with reasoning performance (*age*: $r = -0.04$, $p = 0.75$; *gender*: $t = 1.01$, $p = 0.32$). We first ran two-sample t-tests to assess whether the number of components in each hemisphere (*two* vs *less than two*) related to reasoning performance (Penn Progressive Matrices Test). Next, to determine if the presence of a specific pimfs component was related to reasoning performance, we ran additional two-sample t-tests to test for an effect of presence of the pimfs-v and pimfs-d (*present* vs *absent*) in each hemisphere. As presented below, this model revealed that the presence of left pimfs-v was linked to reasoning performance. To determine whether this result was impacted by differences in sample size between participants with and without this sulcus, we iteratively sampled a subset of participants from the left pimfs-v present group (N = 57) to match that of the left pimfs-v absent group (N = 14) 1000 times and conducted a Welch's t-test for each sampling (to account for the distributions potentially being unequal when resampling). To evaluate the results, we report the median and 95% confidence interval for the effect size.

To ascertain whether the observed relationship between sulcal morphology and cognition is specific to reasoning performance, or generalizable to other measures of cognitive processing, we tested this sulcal-behavior relationship with measures of processing speed (Pattern Comparison Processing Speed Test) and working memory (List Sorting Working Memory Test). Participant age and gender were not considered in these analyses, as they were not reliably associated with processing speed (*age*: $r = -0.21$, $p = 0.08$; *gender*: $t = 0.06$, $p = 0.95$) or working memory (*age*: $r = -0.03$, $p = 0.81$; *gender*: $t = 1.59$, $p = 0.12$). Two-sample t-tests were run to assess for differences in performance on each measure based on left pimfs-v presence (*present* vs *absent*). If either test showed a strong association, we then used the Akaike Information Criterion (AIC) to compare the model predictions to reasoning predictions. Briefly, the AIC provides an estimate of in-sample prediction error and is suitable for non-nested model comparison. By comparing AIC scores, we are able to assess the relative performance of the two models. If the ΔAIC is >2, it suggests an interpretable difference between models. If the ΔAIC is >10, it suggests a strong difference between models, with the lower AIC value indicating the preferred model [61,62].

T-tests were implemented with the t.test function from the R stats package. T-test effect sizes are reported with the Cohen's d (d) metric. The median and 95% confidence intervals were calculated with the MedianCI function from the DescTools R package. AIC values were quantified with the AIC function from the stats R package.

(f) <u>Probability maps</u>

As in prior work [23,25,29,30,63], sulcal probability maps were calculated to display the vertices with the highest alignment across participants for a given sulcus. To generate these maps, the label file for each pimfs component was transformed from the individual to the fsaverage surface. Once transformed into this common template space, we calculated, for each vertex, the proportion of participants for whom the vertex is labeled as the given pimfs component. For vertices where the pimfs components overlapped, we employed a greedy, "winner-take-all" approach such that the component with the highest overlap across participants was assigned to a given vertex. In addition to providing unthresholded maps, we also constrain these maps to maximum probability maps (MPMs) at 10% and 20% participant overlap to increase interpretability (10% overlap MPMs are shown in **figure 3**).

Results

Anatomical and behavioral data were randomly selected from 72 participants (50% female, aged 22-36) from the HCP study [64]. Cortical reconstructions were then generated from T1-weighted MRI scans using FreeSurfer [31,32,49]. Following previously established criteria and the definition of 2,877 sulci across 144 hemispheres (**Materials and Methods**), we manually defined the component(s) of the pimfs, when present. Four example hemispheres are presented in **figure 1**. Analyses on the patterning of the pimfs found that it was more common for young adults to have two components in a given hemisphere (*left*: 72.22% of participants; *right*: 77.78%) than either one (*left*: 25%; *right*: 20.83%) or none (*left*: 2.78%; *right*: 1.39%; $\chi^2 > 54$, $p < 1.50e-12$

in both hemispheres). There was no hemispheric asymmetry in incidence rates (*p* = 0.66; **figure 1**), and when only one pimfs component was present, it was equally likely to be a dorsal or ventral component ($\chi^2 < 2$, $p > .15$ in both hemispheres; **figure 1**). These incidence rates were similar to those observed in children and adolescents [24], which was anticipated given that sulci are formed during gestation [3,12,55,65,66].

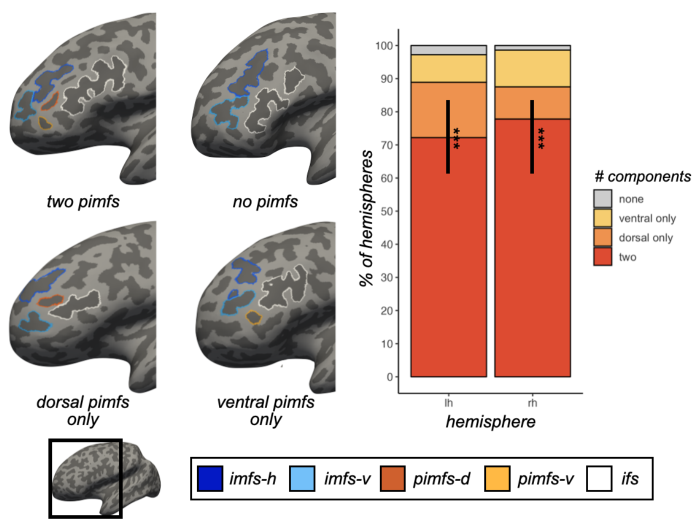

Figure 1. The incidence of the pimfs is highly variable across individuals and hemispheres. *Left:* Inflated left hemispheres (sulci: dark gray; gyri: light gray; cortical surfaces are not to scale) depicting the four types of the para-intermediate frontal sulcus (pimfs): (i) both components present, (ii) neither present, (iii) dorsal component present, (iv) ventral component present. The prominent sulci bounding the pimfs are also shown: the horizontal (imfs-h) and ventral (imfs-v) intermediate frontal sulci and inferior frontal sulcus (ifs). Each sulcus is colored according to the bottom legend. *Right:* Stacked bar plot depicting the incidence of the pimfs components in both the left (lh) and right (rh) hemispheres across the sample of 72 young adults. Each type of the pimfs is colored according to the rightward legend. (***, $p < .001$)

As the pimfs is variably present among young adults, we statistically tested whether this variability was related to reasoning performance, as previously found for children and adolescents [24]. Reasoning performance was quantified as scores on the Penn Progressive Matrices Test from the NIH Toolbox [34], a relational reasoning task similar to the WISC-IV Matrix Reasoning task used previously [23,24,40]. The presence of two pimfs components in the left hemisphere was associated with 21% better reasoning performance relative to either one or none ($t(69) = 2.54$, $p = 0.01$, $d = 0.67$). We had found previously in children and adolescents that this effect was driven by the presence or absence of the left hemisphere pimfs-v [24]. Here, we find that this is also true in young adults. The presence of left pimfs-v was associated with 34% higher reasoning scores ($t(69) = 3.44$, $p = 0.001$, $d = 1.03$; **figure 2*a***); no other pimfs component in either hemisphere showed this effect (ts < 1.32, ps > 0.19, *d*s < 0.47). To account for the difference in sample sizes between adults with and without the left pimfs-v, we iteratively sampled a size-matched subset of the left pimfs-v present group 1000 times. This procedure confirmed the behavioral difference (median, 95% CI d = 0.92, 0.90-0.94; **figure 2*b***).

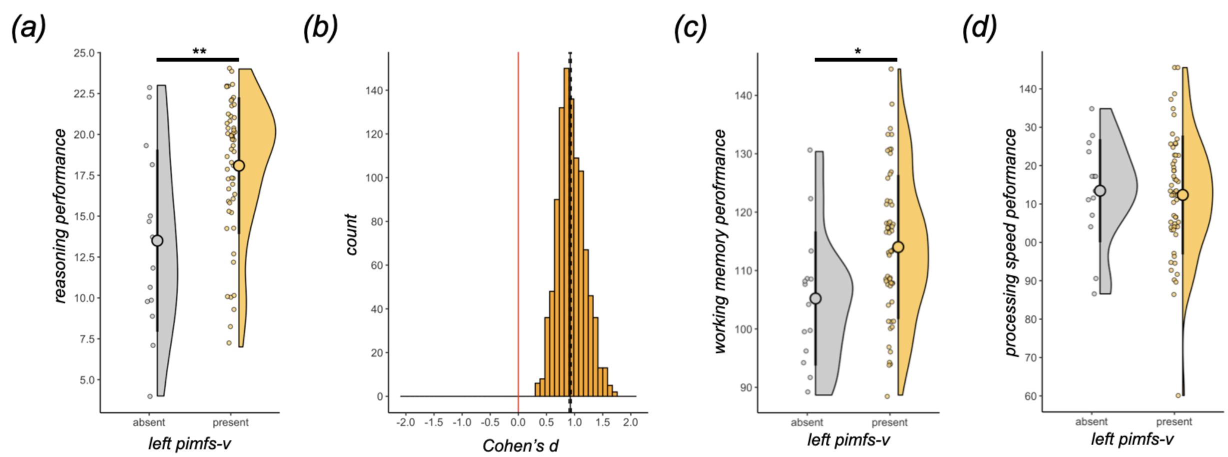

Figure 2. The presence of the para-intermediate frontal sulcus is related to relational thinking. *(a)* Raincloud plots [67] depicting Penn Progressive Matrices task score as a function of left pimfs-v presence in young adults (present, N = 57; absent, N = 14). The large dots and error bars represent the mean ± std reasoning score, and the violin plots show the kernel density estimate. The smaller dots indicate individual participants. *(b)* Histogram visualizing the results of the iterative resampling of the left pimfs-v present group in (A) 1000 times. The distribution of the effect size (Cohen's d) is shown, along with the median (black line) and 95% CI (dotted lines). The red line corresponds to zero to emphasize that none of the comparisons ever showed a reverse relationship in reasoning scores (i.e., left pimfs-v absent having higher reasoning scores than left pimfs-v present). *(c)* Same format as *(a)* for the List Sorting task. *(d)* Same format as *(a)* for the Pattern Completion task. (**, $p < .01$; *, $p < .05$)

Finally, to assess the generalizability and/or specificity of this brain-behavior relationship, we tested whether the presence of left pimfs-v was associated with performance on tests of working memory (WM; List Sorting Working Memory Test) and/or processing speed (Pattern Comparison Processing Speed Test), foundational cognitive skills that support reasoning [68–

72]. As noted above, the WM test administered to HCP participants involves reordering items according to their relative size, thereby placing demands on relational thinking (**Materials and Methods**). Left pimfs-v presence was positively associated with 9% better performance on the WM test (t(69) = 2.42, p = 0.01, *d* = 0.72; **figure 2*c***). While this effect was significant, it was not as large as that observed for the reasoning test ($\Delta AIC_{(working\ memory\ -\ reasoning)}$ = 142.23). By contrast, left pimfs-v presence was not related to processing speed test performance (t(69) = -0.24, p = 0.81, *d* = -0.07**; figure 2*d***), a finding suggesting some degree of specificity in this brain–behavior relation and consistent with previous anatomical-cognitive findings in our pediatric cohort [23,24].

Discussion

Integrating these data with prior work, at least one pimfs component is identifiable in the majority of human hemispheres [277/288 (96%)], with comparable incidence between young adults [141/144 (97%)] and children and adolescents [136/144 (94%)] [24]. However, these incidence rates are in stark contrast to what is observed in chimpanzees [2/60 (3%; one chimpanzee)] [25], emphasizing that the pimfs is a largely human-specific cortical structure. Further, this structure exhibits prominent variability in humans that is robustly linked to variability in reasoning performance, both in young adulthood (ages 22-36), as reported here, and in childhood and adolescence (ages 6-18) [24]. Considering that smaller, shallower (tertiary) sulci in association cortices, such as the pimfs, develop later in gestation than larger, deeper sulci like the central and calcarine sulci [65,66,73], a testable evolutionary and developmental hypothesis is that the higher incidence of the pimfs in humans — and cortical sulci in general [25,29,57,74] — is a consequence of the markedly protracted and greater intrauterine brain growth generally seen in humans compared to chimpanzees [75].

With regard to the relationship to reasoning performance, it is notable that the pimfs-v appears to co-localize with rostrolateral PFC (RLPFC), a functionally defined region consistently implicated in a variety of reasoning tasks by both neuropsychological and fMRI studies [19,72,76–81], including matrix reasoning tasks like the one used in the present study [42,82,83]. Tightly controlled fMRI studies have also pointed to the left RLPFC as playing a particularly strong role in relational thinking [72,84]. However, precise localization of RLPFC at the individual level has been impeded by normalization and group averaging of fMRI activation. As such, future work should assess whether the pimfs-v is a useful landmark that predicts the location of functionally defined RLPFC in individual participants, given that other sulci in association cortices have been identified as functional landmarks [29,85–89].

The extensive variability in the presence/absence of the pimfs components across individuals, and the rarity of the pimfs in chimpanzees, likely also reflects differences in white matter architecture. For example, RLPFC is disproportionately expanded in humans relative to non-human primates, which has been hypothesized to contribute to species differences in reasoning capacity [77,90]. Further, the presence/absence and morphology of sulci are theorized to be anatomically linked to cortical white matter [12,14,30,91–93]. Given that the pimfs is rare in chimpanzees [25], the presence of left pimfs-v could reflect evolutionarily expanded white matter properties that enhance neural communication in this higher cognitive area [3,13–15]. Tentatively supporting this idea, the white matter properties and functional connectivity of long-range connections involving RLPFC have been linked to reasoning performance and developmental growth [94]. Future research should investigate this multiscale, mechanistic relationship describing the neural correlates of reasoning, integrating structural, functional, and behavioral data.

In this young adult sample, we showed that the presence of left pimfs-v was associated not only with 34% (on average) better performance on a test of relational reasoning, but also 9% (on average) better performance on a test of WM that requires relational thinking. On the other hand, this sulcal feature was unrelated to processing speed. In our pediatric sample, the presence of left pimfs-v was not related either to processing speed or to WM. In that prior study, the test of

WM was a standard measure that involves repeating a series of digits in either the forward or reverse order (WISC-IV Digit Span task) [40]. Given that participants in the two samples completed different WM tasks, it is an open question whether presence/absence of the pimfs-v is only linked to WM when the task requires relational thinking — a plausible hypothesis, given that RLPFC is not thought to be centrally involved in WM per se (e.g., [47,48]). Future research should further explore the specificity of the cognitive effects of presence/absence of the left pimfs-v, as well as test whether and how the presence/absence of the right pimfs-v and left/right pimfs-d are cognitively relevant in other domains.

To date, the patterning and cognitive relevance of the pimfs has only been examined in neurotypical populations [23,24,56]. Numerous studies of disorders such as schizophrenia, autism spectrum disorder, obsessive-compulsive disorder, and fronto-temporal dementia have found that variations in sulcal incidence are clinically relevant — although most of this work has focused on the ACC (e.g., [95–103]) and orbitofrontal cortex (for review see [104]). Thus, the present results raise the question of whether the incidence of the pimfs differs in any of the clinical populations that exhibit impaired reasoning. Schizophrenia is a prime candidate for future investigations, given that it is marked by impaired reasoning [105–110] and has repeatedly been associated with altered RLPFC structure and function [111–117]. To help guide future studies examining the cognitive, evolutionary, developmental, clinical, and functional relevance of the pimfs, we share probabilistic predictions of the pimfs from our data (**figure 3**; **Data accessibility**).

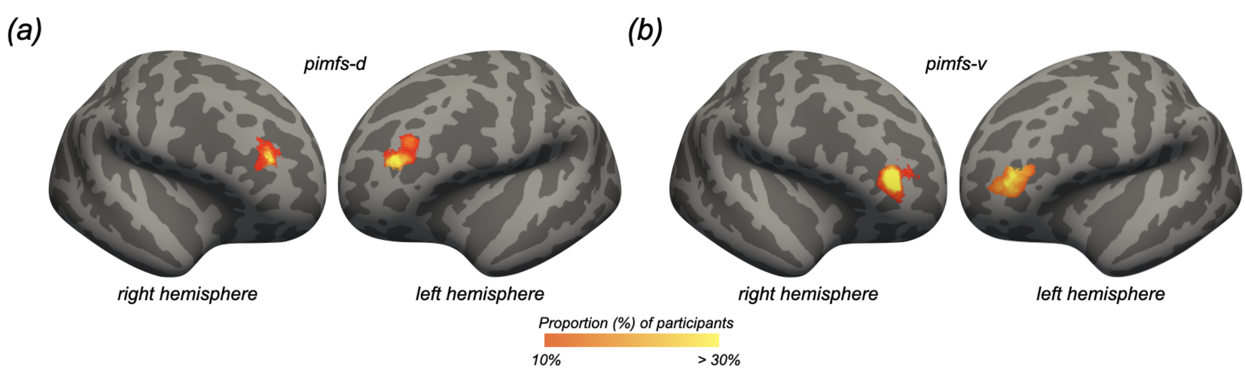

Figure 3. Maximum probability maps for the para-intermediate frontal sulcus. Maximum probability maps (MPMs) for the pimfs-d *(a)* and pimfs-v *(b)* overlayed on the inflated fsaverage cortical surface (sulci: dark gray; gyri: light gray; cortical surfaces are not to scale). To generate the MPMs, each label was transformed from each individual to the fsaverage surface. For each vertex, the proportion of participants for whom that vertex is labeled as the given sulcus (the warmer the color, the higher the overlap) was calculated. In the cases in which the vertices for each component overlapped, the sulcus with the highest overlap across participants was assigned to that vertex. For visual clarity, the MPMs were thresholded to 10% overlap across participants.

In conclusion, we have extended prior work in children and adolescents [24] by showing that the presence of the left hemisphere pimfs-v is also cognitively relevant in young adulthood. The combination of findings across studies empirically shows that the presence/absence of the pimfs-v is a novel developmental, cognitive, and evolutionarily relevant feature that should be considered in future studies in neurotypical and clinical populations examining how the complex relationships among multiscale anatomical and functional features of the brain give rise to abstract thought.

Ethics statement

HCP consortium data were previously acquired using protocols approved by the Washington University Institutional Review Board.

Competing interests statement

The authors declare no competing financial interests.

Data accessibility statement

Data, analysis pipelines, and pimfs probability maps will be made freely available on GitHub upon publication (https://github.com/cnl-berkeley/stable_projects/). Requests for further information or raw data should be directed to the Corresponding Author, Kevin S. Weiner (kweiner@berkeley.edu).

Author contributions statement

EHW, SAB, and KSW designed research; EHW, SJ, SC, CBH, WIV, and KSW performed manual sulcal labeling; EHW, SAB, and KSW analyzed data; EHW, SAB, and KSW wrote the paper; all authors gave final approval to the paper before submission.

Funding information

This research was supported by NICHD R21HD100858 (Weiner, Bunge), an NSF CAREER Award 2042251 (Weiner), and an NSF-GRFP fellowship (Voorhies). Young adult neuroimaging and behavioral data were provided by the HCP, WU-Minn Consortium (Principal Investigators: David Van Essen and Kamil Ugurbil; NIH Grant 1U54-MH-091657) funded by the 16 NIH Institutes and Centers that support the NIH Blueprint for Neuroscience Research, and the McDonnell Center for Systems Neuroscience at Washington University.

Acknowledgments

We thank Jewelia Yao and Jacob Miller for their assistance defining other additional lateral prefrontal cortex sulci across age groups. We also thank the HCP researchers for participant recruitment and data collection and sharing, as well as the participants who took part in the study.

References

1. Van Essen DC. 2007 4.16 - Cerebral Cortical Folding Patterns in Primates: Why They Vary and What They Signify. In *Evolution of Nervous Systems* (ed JH Kaas), pp. 267–276. Oxford: Academic Press.

2. Zilles K, Armstrong E, Schleicher A, Kretschmann H-J. 1988 The human pattern of gyrification in the cerebral cortex. *Anatomy and Embryology*. **179**, 173–179. (doi:10.1007/bf00304699)

3. Zilles K, Palomero-Gallagher N, Amunts K. 2013 Development of cortical folding during evolution and ontogeny. *Trends Neurosci.* **36**, 275–284.

4. Yousry TA, Schmid UD, Alkadhi H, Schmidt D, Peraud A, Buettner A, Winkler P. 1997 Localization of the motor hand area to a knob on the precentral gyrus. A new landmark. *Brain* **120 (Pt 1)**, 141–157.

5. Boling W, Olivier A, Bittar RG, Reutens D. 1999 Localization of hand motor activation in Broca's pli de passage moyen. *J. Neurosurg.* **91**, 903–910.

6. Hinds OP *et al.* 2008 Accurate prediction of V1 location from cortical folds in a surface coordinate system. *Neuroimage* **39**, 1585–1599.

7. Cykowski MD, Coulon O, Kochunov PV, Amunts K, Lancaster JL, Laird AR, Glahn DC, Fox PT. 2008 The central sulcus: an observer-independent characterization of sulcal landmarks and depth asymmetry. *Cereb. Cortex* **18**, 1999–2009.

8. Li S *et al.* 2010 Mapping surface variability of the central sulcus in musicians. *Cereb. Cortex* **20**, 25–33.

9. Wandell BA, Winawer J. 2011 Imaging retinotopic maps in the human brain. *Vision Res.* **51**, 718–737.

10. Benson NC, Butt OH, Datta R, Radoeva PD, Brainard DH, Aguirre GK. 2012 The retinotopic organization of striate cortex is well predicted by surface topology. *Curr. Biol.* **22**, 2081–2085.

11. Sun ZY, Klöppel S, Rivière D, Perrot M, Frackowiak R, Siebner H, Mangin J-F. 2012 The effect of handedness on the shape of the central sulcus. *Neuroimage* **60**, 332–339.

12. Cachia A, Borst G, Jardri R, Raznahan A, Murray GK, Mangin J-F, Plaze M. 2021 Towards Deciphering the Fetal Foundation of Normal Cognition and Cognitive Symptoms From Sulcation of the Cortex. *Front. Neuroanat.* **15**, 712862.

13. Van Essen DC. 1997 A tension-based theory of morphogenesis and compact wiring in the central nervous system. *Nature* **385**, 313–318.

14. Van Essen DC. 2020 A 2020 view of tension-based cortical morphogenesis. *Proc. Natl. Acad. Sci. U. S. A.* (doi:10.1073/pnas.2016830117)

15. White T, Su S, Schmidt M, Kao C-Y, Sapiro G. 2010 The development of gyrification in childhood and adolescence. *Brain Cogn.* **72**, 36–45.

16. Luria AR. 1966 *Higher Cortical Functions in Man*. Springer US.

17. Milner B, Petrides M. 1984 Behavioural effects of frontal-lobe lesions in man. *Trends Neurosci.* **7**, 403–407.

18. Stuss DT, Knight RT. 2013 *Principles of Frontal Lobe Function*. OUP USA.

19. Urbanski M *et al.* 2016 Reasoning by analogy requires the left frontal pole: lesion-deficit mapping and clinical implications. *Brain* **139**, 1783–1799.

20. Donahue CJ, Glasser MF, Preuss TM, Rilling JK, Van Essen DC. 2018 Quantitative assessment of prefrontal cortex in humans relative to nonhuman primates. *Proc. Natl. Acad. Sci. U. S. A.* **115**, E5183–E5192.

21. Smaers JB, Gómez-Robles A, Parks AN, Sherwood CC. 2017 Exceptional Evolutionary Expansion of Prefrontal Cortex in Great Apes and Humans. *Curr. Biol.* **27**, 714–720.

22. Smaers JB *et al.* 2021 The evolution of mammalian brain size. *Sci Adv* **7**. (doi:10.1126/sciadv.abe2101)

23. Voorhies WI, Miller JA, Yao JK, Bunge SA, Weiner KS. 2021 Cognitive insights from tertiary sulci in prefrontal cortex. *Nat. Commun.* **12**, 5122.

24. Willbrand EH, Voorhies WI, Yao JK, Weiner KS, Bunge SA. 2022 Presence or absence of a prefrontal sulcus is linked to reasoning performance during child development. *Brain Struct. Funct.* **227**, 2543–2551.

25. Hathaway CB, Voorhies WI, Sathishkumar N, Mittal C, Yao JK, Miller JA, Parker BJ, Weiner KS. 2022 Defining tertiary sulci in lateral prefrontal cortex in chimpanzees using human predictions. *bioRxiv*. , 2022.04.12.488091. (doi:10.1101/2022.04.12.488091)

26. Marek S *et al.* 2022 Reproducible brain-wide association studies require thousands of individuals. *Nature* **603**, 654–660.

27. Gratton C, Nelson SM, Gordon EM. 2022 Brain-behavior correlations: Two paths toward reliability. *Neuron*. **110**, 1446–1449.

28. Westlin C *et al.* 2023 Improving the study of brain-behavior relationships by revisiting basic assumptions. *Trends Cogn. Sci.* (doi:10.1016/j.tics.2022.12.015)

29. Willbrand EH *et al.* 2022 Uncovering a tripartite landmark in posterior cingulate cortex. *Science Advances* **8**, eabn9516.

30. Miller JA, Voorhies WI, Lurie DJ, D'Esposito M, Weiner KS. 2021 Overlooked Tertiary Sulci Serve as a Meso-Scale Link between Microstructural and Functional Properties of Human Lateral Prefrontal Cortex. *J. Neurosci.* **41**, 2229–2244.

31. Dale AM, Fischl B, Sereno MI. 1999 Cortical surface-based analysis. I. Segmentation and surface reconstruction. *Neuroimage* **9**, 179–194.

32. Fischl B, Sereno MI, Dale AM. 1999 Cortical surface-based analysis. II: Inflation, flattening, and a surface-based coordinate system. *Neuroimage* **9**, 195–207.

33. Glasser MF *et al.* 2013 The minimal preprocessing pipelines for the Human Connectome Project. *Neuroimage* **80**, 105–124.

34. Barch DM *et al.* 2013 Function in the human connectome: task-fMRI and individual differences in behavior. *Neuroimage* **80**, 169–189.

35. James W. 1890 The principles of psychology, Vol I. (doi:10.1037/10538-000)

36. James W. 1890 The Principles Of Psychology Volume II By William James (1890).

37. Cattell RB. 1943 The measurement of adult intelligence. *Psychol. Bull.* **40**, 153–193.

38. Alexander PA. 2016 Relational thinking and relational reasoning: harnessing the power of patterning. *NPJ Sci Learn* **1**, 16004.

39. Raven JC. 1941 Standardization of progressive matrices, 1938. *Br. J. Med. Psychol.* **19**, 137–150.

40. Wechsler D. 1949 Wechsler Intelligence Scale for Children; manual. **113**.

41. Prabhakaran V, Smith JA, Desmond JE, Glover GH, Gabrieli JD. 1997 Neural substrates of fluid reasoning: an fMRI study of neocortical activation during performance of the Raven's Progressive Matrices Test. *Cogn. Psychol.* **33**, 43–63.

42. Christoff K, Prabhakaran V, Dorfman J, Zhao Z, Kroger JK, Holyoak KJ, Gabrieli JD. 2001 Rostrolateral prefrontal cortex involvement in relational integration during reasoning. *Neuroimage* **14**, 1136–1149.

43. Conway ARA, Kane MJ, Bunting MF, Hambrick DZ, Wilhelm O, Engle RW. 2005 Working memory span tasks: A methodological review and user's guide. *Psychon. Bull. Rev.* **12**, 769–786.

44. Gray JR, Chabris CF, Braver TS. 2003 Neural mechanisms of general fluid intelligence. *Nat. Neurosci.* **6**, 316–322.

45. Gray JR, Burgess GC, Schaefer A, Yarkoni T, Larsen RJ, Braver TS. 2005 Affective personality differences in neural processing efficiency confirmed using fMRI. *Cogn. Affect. Behav. Neurosci.* **5**, 182–190.

46. Wendelken C, Nakhabenko D, Donohue SE, Carter CS, Bunge SA. 2008 'Brain is to thought as stomach is to ??': investigating the role of rostrolateral prefrontal cortex in relational reasoning. *J. Cogn. Neurosci.* **20**, 682–693.

47. Wendelken C, Bunge SA, Carter CS. 2008 Maintaining structured information: an investigation into functions of parietal and lateral prefrontal cortices. *Neuropsychologia* **46**, 665–678.

48. Wendelken C, Bunge SA. 2010 Transitive inference: distinct contributions of rostrolateral prefrontal cortex and the hippocampus. *J. Cogn. Neurosci.* **22**, 837–847.

49. Fischl B, Sereno MI, Tootell RB, Dale AM. 1999 High-resolution intersubject averaging and a coordinate system for the cortical surface. *Hum. Brain Mapp.* **8**, 272–284.

50. Wandell BA, Chial S, Backus BT. 2000 Visualization and measurement of the cortical surface. *J. Cogn. Neurosci.* **12**, 739–752.

51. Weiner KS, Natu VS, Grill-Spector K. 2018 On object selectivity and the anatomy of the human fusiform gyrus. *Neuroimage* **173**, 604–609.

52. Edlow BL *et al.* 2019 7 Tesla MRI of the ex vivo human brain at 100 micron resolution. *Sci Data* **6**, 244.

53. Lüsebrink F, Sciarra A, Mattern H, Yakupov R, Speck O. 2017 T1-weighted in vivo human whole brain MRI dataset with an ultrahigh isotropic resolution of 250 μm. *Sci Data* **4**, 170032.

54. Weiner KS, Golarai G, Caspers J, Chuapoco MR, Mohlberg H, Zilles K, Amunts K, Grill-Spector K. 2014 The mid-fusiform sulcus: a landmark identifying both cytoarchitectonic and functional divisions of human ventral temporal cortex. *Neuroimage* **84**, 453–465.

55. Miller JA, D'Esposito M, Weiner KS. 2021 Using Tertiary Sulci to Map the 'Cognitive Globe' of Prefrontal Cortex. *J. Cogn. Neurosci.* , 1–18.

56. Yao JK, Voorhies WI, Miller JA, Bunge SA, Weiner KS. 2022 Sulcal depth in prefrontal cortex: a novel predictor of working memory performance. *Cereb. Cortex* , bhac173.

57. Petrides M. 2019 *Atlas of the Morphology of the Human Cerebral Cortex on the Average MNI Brain*. Academic Press.

58. Petrides M. 2013 *Neuroanatomy of Language Regions of the Human Brain*. Academic Press.

59. Borne L, Rivière D, Mancip M, Mangin J-F. 2020 Automatic labeling of cortical sulci using patch- or CNN-based segmentation techniques combined with bottom-up geometric constraints. *Med. Image Anal.* **62**, 101651.

60. Willbrand EH, Ferrer E, Bunge SA, Weiner KS. 2022 Development of human lateral prefrontal sulcal morphology and its relation to reasoning performance. *bioRxiv*. , 2022.09.14.507822. (doi:10.1101/2022.09.14.507822)

61. Wagenmakers E-J, Farrell S. 2004 AIC model selection using Akaike weights. *Psychon. Bull. Rev.* **11**, 192–196.

62. Burnham KP, Anderson DR. 2004 Multimodel Inference: Understanding AIC and BIC in Model Selection. *Sociol. Methods Res.* **33**, 261–304.

63. Miller JA, Voorhies WI, Li X, Raghuram I, Palomero-Gallagher N, Zilles K, Sherwood CC, Hopkins WD, Weiner KS. 2020 Sulcal morphology of ventral temporal cortex is shared between humans and other hominoids. *Sci. Rep.* **10**, 17132.

64. Van Essen DC *et al.* 2012 The Human Connectome Project: a data acquisition perspective. *Neuroimage* **62**, 2222–2231.

65. Chi JG, Dooling EC, Gilles FH. 1977 Gyral development of the human brain. *Ann. Neurol.* **1**, 86–93.

66. Armstrong E, Schleicher A, Omran H, Curtis M, Zilles K. 1995 The ontogeny of human gyrification. *Cereb. Cortex* **5**, 56–63.

67. Allen M, Poggiali D, Whitaker K, Marshall TR, van Langen J, Kievit RA. 2021 Raincloud plots: a multi-platform tool for robust data visualization. *Wellcome Open Res.* **4**, 63.

68. Fry AF, Hale S. 2000 Relationships among processing speed, working memory, and fluid intelligence in children. *Biol. Psychol.* **54**, 1–34.

69. Ferrer E, Whitaker KJ, Steele JS, Green CT, Wendelken C, Bunge SA. 2013 White matter maturation supports the development of reasoning ability through its influence on processing speed. *Dev. Sci.* **16**, 941–951.

70. Kail R, Salthouse TA. 1994 Processing speed as a mental capacity. *Acta Psychol.* **86**, 199–225.

71. Kail RV, Lervåg A, Hulme C. 2016 Longitudinal evidence linking processing speed to the development of reasoning. *Dev. Sci.* **19**, 1067–1074.

72. Holyoak KJ, Monti MM. 2021 Relational Integration in the Human Brain: A Review and Synthesis. *Journal of Cognitive Neuroscience*. **33**, 341–356. (doi:10.1162/jocn_a_01619)

73. Welker W. 1990 Why Does Cerebral Cortex Fissure and Fold? In *Cerebral Cortex: Comparative Structure and Evolution of Cerebral Cortex, Part II* (eds EG Jones, A Peters), pp. 3–136. Boston, MA: Springer US.

74. Amiez C, Sallet J, Hopkins WD, Meguerditchian A, Hadj-Bouziane F, Ben Hamed S, Wilson CRE, Procyk E, Petrides M. 2019 Sulcal organization in the medial frontal cortex provides insights into primate brain evolution. *Nat. Commun.* **10**, 1–14.

75. Sakai T *et al.* 2012 Fetal brain development in chimpanzees versus humans. *Curr. Biol.* **22**, R791–2.

76. Krawczyk DC. 2012 The cognition and neuroscience of relational reasoning. *Brain Res.* **1428**, 13–23.

77. Vendetti MS, Bunge SA. 2014 Evolutionary and developmental changes in the lateral frontoparietal network: a little goes a long way for higher-level cognition. *Neuron* **84**, 906–917.

78. Aichelburg C, Urbanski M, Thiebaut de Schotten M, Humbert F, Levy R, Volle E. 2016 Morphometry of Left Frontal and Temporal Poles Predicts Analogical Reasoning Abilities. *Cereb. Cortex* **26**, 915–932.

79. Hobeika L, Diard-Detoeuf C, Garcin B, Levy R, Volle E. 2016 General and specialized brain correlates for analogical reasoning: A meta-analysis of functional imaging studies. *Hum. Brain Mapp.* **37**, 1953–1969.

80. Hartogsveld B, Bramson B, Vijayakumar S, van Campen AD, Marques JP, Roelofs K, Toni I, Bekkering H, Mars RB. 2018 Lateral frontal pole and relational processing: Activation patterns and connectivity profile. *Behav. Brain Res.* **355**, 2–11.

81. Assem M, Glasser MF, Van Essen DC, Duncan J. 2020 A Domain-General Cognitive Core

Defined in Multimodally Parcellated Human Cortex. *Cereb. Cortex* **30**, 4361–4380.

82. Kroger JK, Sabb FW, Fales CL, Bookheimer SY, Cohen MS, Holyoak KJ. 2002 Recruitment of anterior dorsolateral prefrontal cortex in human reasoning: a parametric study of relational complexity. *Cereb. Cortex* **12**, 477–485.

83. Crone EA, Wendelken C, van Leijenhorst L, Honomichl RD, Christoff K, Bunge SA. 2009 Neurocognitive development of relational reasoning. *Dev. Sci.* **12**, 55–66.

84. Bunge SA, Helskog EH, Wendelken C. 2009 Left, but not right, rostrolateral prefrontal cortex meets a stringent test of the relational integration hypothesis. *Neuroimage* **46**, 338–342.

85. Weiner KS. 2019 The Mid-Fusiform Sulcus (sulcus sagittalis gyri fusiformis). *Anat. Rec.* **302**, 1491–1503.

86. Lopez-Persem A, Verhagen L, Amiez C, Petrides M, Sallet J. 2019 The Human Ventromedial Prefrontal Cortex: Sulcal Morphology and Its Influence on Functional Organization. *J. Neurosci.* **39**, 3627–3639.

87. Amiez C, Petrides M. 2014 Neuroimaging evidence of the anatomo-functional organization of the human cingulate motor areas. *Cereb. Cortex* **24**, 563–578.

88. Amiez C, Neveu R, Warrot D, Petrides M, Knoblauch K, Procyk E. 2013 The location of feedback-related activity in the midcingulate cortex is predicted by local morphology. *J. Neurosci.* **33**, 2217–2228.

89. Li Y, Sescousse G, Amiez C, Dreher J-C. 2015 Local morphology predicts functional organization of experienced value signals in the human orbitofrontal cortex. *J. Neurosci.* **35**, 1648–1658.

90. Semendeferi K, Armstrong E, Schleicher A, Zilles K, Van Hoesen GW. 2001 Prefrontal cortex in humans and apes: a comparative study of area 10. *Am. J. Phys. Anthropol.* **114**, 224–241.

91. Reveley C, Seth AK, Pierpaoli C, Silva AC, Yu D, Saunders RC, Leopold DA, Ye FQ. 2015 Superficial white matter fiber systems impede detection of long-range cortical connections in diffusion MR tractography. *Proc. Natl. Acad. Sci. U. S. A.* **112**, E2820–8.

92. Sanides F. 1962 Besprechung. In *Die Architektonik des Menschlichen Stirnhirns: Zugleich eine Darstellung der Prinzipien Seiner Gestaltung als Spiegel der Stammesgeschichtlichen Differenzierung der Grosshirnrinde* (ed F Sanides), pp. 176–190. Berlin, Heidelberg: Springer Berlin Heidelberg.

93. Sanides F. 1964 Structure and function of the human frontal lobe. *Neuropsychologia* **2**, 209–219.

94. Wendelken C, Ferrer E, Ghetti S, Bailey SK, Cutting L, Bunge SA. 2017 Frontoparietal Structural Connectivity in Childhood Predicts Development of Functional Connectivity and Reasoning Ability: A Large-Scale Longitudinal Investigation. *J. Neurosci.* **37**, 8549–8558.

95. Yücel M *et al.* 2002 Paracingulate morphologic differences in males with established schizophrenia: a magnetic resonance imaging morphometric study. *Biol. Psychiatry* **52**, 15–

23.

96. Yücel M, Wood SJ, Phillips LJ, Stuart GW, Smith DJ, Yung A, Velakoulis D, Mcgorry PD, Pantelis C. 2003 Morphology of the anterior cingulate cortex in young men at ultra-high risk of developing a psychotic illness. *Br. J. Psychiatry* **182**, 518–524.

97. Le Provost J-B *et al.* 2003 Paracingulate sulcus morphology in men with early-onset schizophrenia. *Br. J. Psychiatry* **182**, 228–232.

98. Fornito A, Malhi GS, Lagopoulos J, Ivanovski B, Wood SJ, Saling MM, Pantelis C, Yücel M. 2008 Anatomical abnormalities of the anterior cingulate and paracingulate cortex in patients with bipolar I disorder. *Psychiatry Research: Neuroimaging*. **162**, 123–132. (doi:10.1016/j.pscychresns.2007.06.004)

99. Fornito A, Yücel M, Wood SJ, Proffitt T, McGorry PD, Velakoulis D, Pantelis C. 2006 Morphology of the paracingulate sulcus and executive cognition in schizophrenia. *Schizophr. Res.* **88**, 192–197.

100. Shim G, Jung WH, Choi J-S, Jung MH, Jang JH, Park J-Y, Choi C-H, Kang D-H, Kwon JS. 2009 Reduced cortical folding of the anterior cingulate cortex in obsessive-compulsive disorder. *J. Psychiatry Neurosci.* **34**, 443–449.

101. Harper L *et al.* 2022 Prenatal Gyrification Pattern Affects Age at Onset in Frontotemporal Dementia. *Cereb. Cortex* (doi:10.1093/cercor/bhab457)

102. Meredith SM *et al.* 2012 Anterior cingulate morphology in people at genetic high-risk of schizophrenia. *Eur. Psychiatry* **27**, 377–385.

103. Gay O, Plaze M, Oppenheim C, Gaillard R, Olié J-P, Krebs M-O, Cachia A. 2017 Cognitive control deficit in patients with first-episode schizophrenia is associated with complex deviations of early brain development. *J. Psychiatry Neurosci.* **42**, 87–94.

104. Nakamura M, Nestor PG, Shenton ME. 2020 Orbitofrontal Sulcogyral Pattern as a Transdiagnostic Trait Marker of Early Neurodevelopment in the Social Brain. *Clin. EEG Neurosci.* **51**, 275–284.

105. Weickert TW, Goldberg TE, Gold JM, Bigelow LB, Egan MF, Weinberger DR. 2000 Cognitive impairments in patients with schizophrenia displaying preserved and compromised intellect. *Arch. Gen. Psychiatry* **57**, 907–913.

106. Bowie CR, Harvey PD. 2006 Cognitive deficits and functional outcome in schizophrenia. *Neuropsychiatr. Dis. Treat.* **2**, 531–536.

107. Keefe RSE, Harvey PD. 2012 Cognitive Impairment in Schizophrenia. In *Novel Antischizophrenia Treatments* (eds MA Geyer, G Gross), pp. 11–37. Berlin, Heidelberg: Springer Berlin Heidelberg.

108. Zhang B, Han M, Tan S, De Yang F, Tan Y, Jiang S, Zhang X, Huang X-F. 2017 Gender differences measured by the MATRICS consensus cognitive battery in chronic schizophrenia patients. *Sci. Rep.* **7**, 11821.

109. Alkan E, Davies G, Evans SL. 2021 Cognitive impairment in schizophrenia: relationships with cortical thickness in fronto-temporal regions, and dissociability from symptom severity.

NPJ Schizophr **7**, 20.

110. McCutcheon RA, Keefe RSE, McGuire PK. 2023 Cognitive impairment in schizophrenia: aetiology, pathophysiology, and treatment. *Mol. Psychiatry* (doi:10.1038/s41380-023-01949-9)

111. Kaplan CM, Saha D, Molina JL, Hockeimer WD, Postell EM, Apud JA, Weinberger DR, Tan HY. 2016 Estimating changing contexts in schizophrenia. *Brain* **139**, 2082–2095.

112. Shinba T, Kariya N, Matsuda S, Arai M, Itokawa M, Hoshi Y. 2022 Near-Infrared Time-Resolved Spectroscopy Shows Anterior Prefrontal Blood Volume Reduction in Schizophrenia but Not in Major Depressive Disorder. *Sensors* **22**. (doi:10.3390/s22041594)

113. Nazli ŞB, Koçak OM, Kirkici B, Sevındık M, Kokurcan A. 2020 Investigation of the Processing of Noun and Verb Words with fMRI in Patients with Schizophrenia. *Noro Psikiyatr Ars* **57**, 9–14.

114. Tu P-C, Hsieh J-C, Li C-T, Bai Y-M, Su T-P. 2012 Cortico-striatal disconnection within the cingulo-opercular network in schizophrenia revealed by intrinsic functional connectivity analysis: a resting fMRI study. *Neuroimage* **59**, 238–247.

115. Pillinger T, Rogdaki M, McCutcheon RA, Hathway P, Egerton A, Howes OD. 2019 Altered glutamatergic response and functional connectivity in treatment resistant schizophrenia: the effect of riluzole and therapeutic implications. *Psychopharmacology* **236**, 1985–1997.

116. Kang SS, MacDonald AW 3rd, Chafee MV, Im C-H, Bernat EM, Davenport ND, Sponheim SR. 2018 Abnormal cortical neural synchrony during working memory in schizophrenia. *Clin. Neurophysiol.* **129**, 210–221.

117. Barnes MR *et al.* 2011 Transcription and pathway analysis of the superior temporal cortex and anterior prefrontal cortex in schizophrenia. *J. Neurosci. Res.* **89**, 1218–1227.